Development of an analytical transient evacuation model for the fairing jettison process

Michael Woronowicz*

KBR, Inc., 8120 Maple Lawn Blvd., Fulton, Maryland 20759

ABSTRACT

A general, lumped-parameter, control volume equation is developed to describe the rapid loss of pressure associated with a launch vehicle fairing jettison event in its initial phase. Beginning with a general mass conservation statement, a sonic constraint is applied to the expanding gap between receding fairing halves to produce a statement for transient density. This is related to fairing pressure by assuming the expansion may be described by a polytropic process. A generic, single-step, lateral fairing half separation case is created and explored for illustrative purposes.

Keywords: fairing depressurization, jettison, venting

1. INTRODUCTION

The James Webb Space Telescope (JWST) observatory features large expanses of thin membrane sunshield layers.[1] These membranes were carefully folded prior to launch and supported by Unitized Pallet Structures (UPSs) and Membrane Release Devices (MRDs) (Fig. 1a & 1b).[1] Nevertheless, there were concerns about the possibility that residual pressure within the Ariane 5 (A5) launch vehicle (LV) rapidly released during the fairing jettison event could potentially produce overpressure levels high enough to damage these large, delicate fabrications.

Another delicate item was the Thermal Management Subsystem (TMS) comprising a large portion of the Integrated Science Instrument Module (ISIM) envelope. Certain portions of the TMS also consisted of single layer membranes, and originally ISIM was designed to vent only across the aperture of the Aft Optics Subsystem (AOS). Within ISIM are the individual science instruments, and a number of project personnel were interested in assessing how their units might also be affected by fairing jettison.

More generally, thermal engineers design multilayer insulation (MLI) blankets with a certain expected level of radiative performance. It is recognized that certain abrupt depressurization events such as fairing jettison or LV upper stage separation physically disturb some blankets and may affect their effective emissivity.

The purpose of this paper is to develop an analytical expression for fairing pressure evolution during the jettison event, and after some exploration produce an example to describe the overpressure response of a payload subjected to this rapid depressurization.

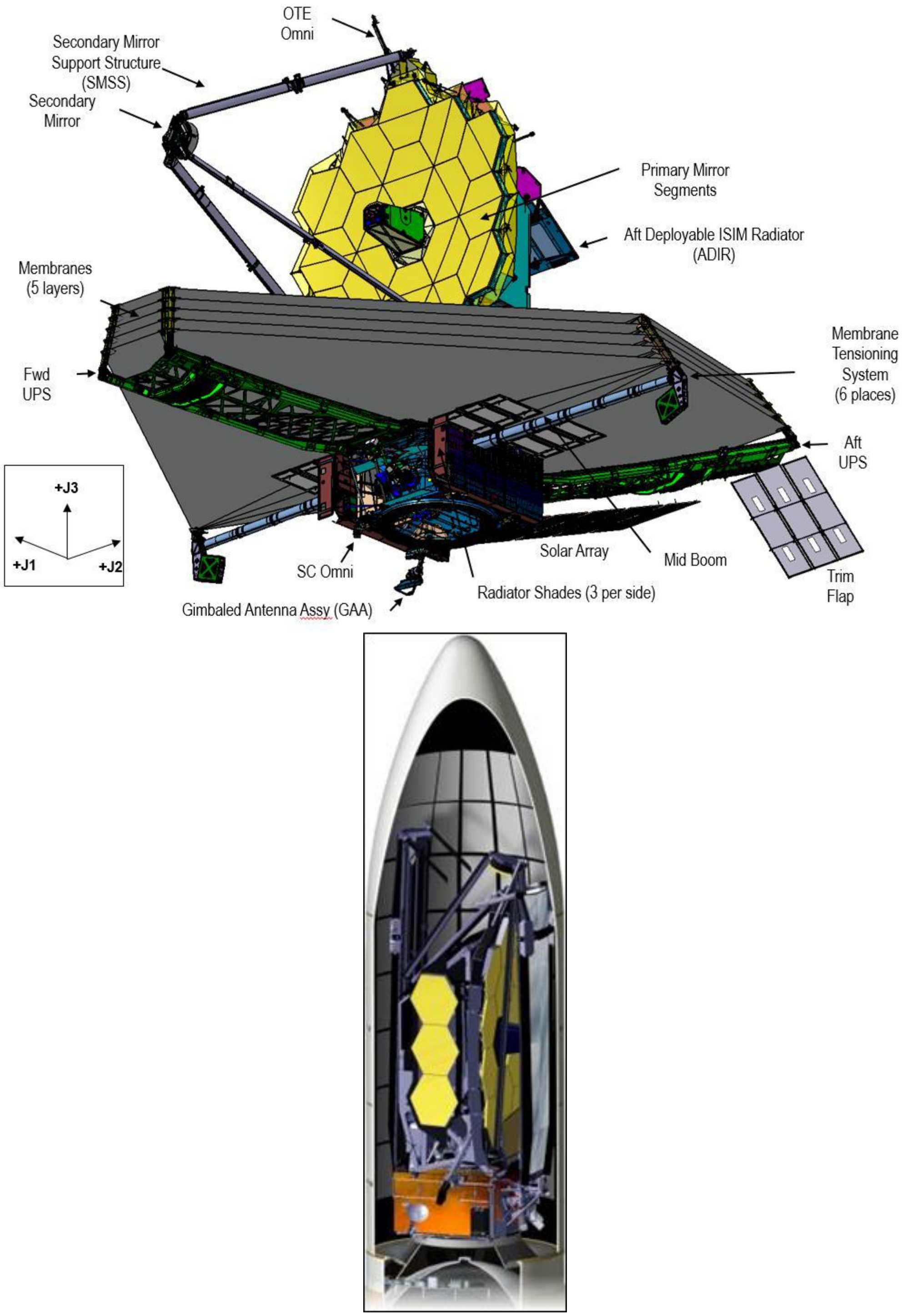

Figure 1. Renderings of JWST (a) with fully deployed Sunshield Membranes and (b) folded up within LV fairing.[1,2]

2. VENTING MASS CONSERVATION STATEMENT

We begin with a statement describing the rate of mass accumulation within volume *V*, made up of the rate of mass generation $\dot{m}_{\text{gen}}$ within *V* minus the net rate at which mass exits across the volume's bounding surface *S*. This system is visualized in Fig. 2.

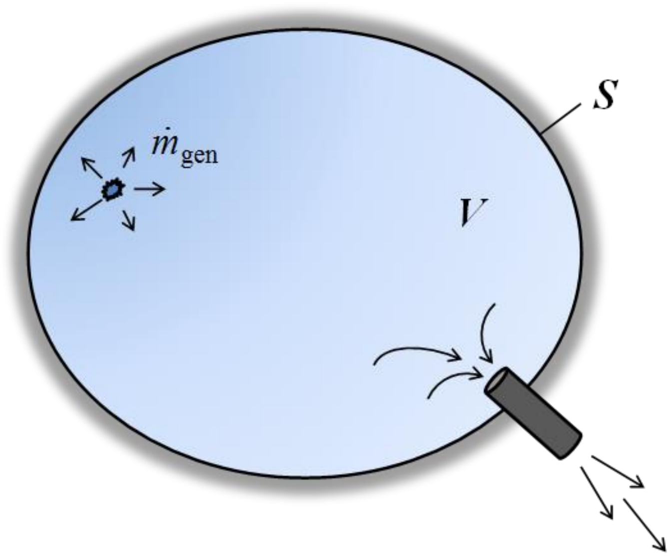

Figure 2. Schematic representation of a simple rigid vessel venting system.

Mass density is given by ρ and u represents flow velocity:

$$\frac{d}{dt}\iiint_V \rho\, dV = \dot{m}_{\text{gen}} - \oiint_S \rho\mathbf{u}\cdot\mathbf{dS}\,. \tag{1}$$

Ignoring the effects of surface desorption and outgassing under continuum conditions, $\dot{m}_{\text{gen}} = 0$. For this control volume analysis, assume fluid properties may be described by lumped parameter conditions. Also for the sake of simplicity, ignore the impact of venting from various payload compartments into the fairing, since their volumes are relatively fairly small with respect to the overall initial fairing volume.

2.1 General Solution

Once the jettison process is initiated, the fairing air density, volume V, and vent area A will all change rapidly with time as the fairing halves separate. The left-hand side of Eq. (1) becomes

$$\frac{\partial}{\partial t}\iiint_V \rho\, dV = V\frac{d\rho}{dt} + \rho\frac{dV}{dt} = \rho V\frac{d}{dt}\left(\ln \rho V\right). \tag{2}$$

Venting from within the fairing to the vacuum of space is constrained by a sonic limit (Mach number $M = 1$, u = sonic velocity $a \equiv \sqrt{\gamma RT} = \sqrt{\frac{2\gamma RT_0}{\gamma+1}}$, and γ represents the ratio of specific heats), therefore the right-hand side of Eq. (1) simplifies to $-\rho aA$ and Eq. (1) itself becomes

$$\frac{d}{dt}\left(\ln \rho V\right) = -\frac{aA}{V}. \tag{3}$$

Integration of Eq. (3) yields

$$\frac{\rho}{\rho_0} = \frac{V_0}{V}\exp\left(-a\int_0^t \frac{A(t)}{V(t)}dt\right). \tag{4}$$

Since the jettison process occurs very rapidly, it was originally thought that heat transfer to the gas over that period would be negligible and the process could be considered isentropic. Fairing pressure may then be related to density by $p \propto \rho^k$, where k is the polytropic exponent. For an isentropic jettison process with zero heat transfer, $k = \gamma$, while at the other end of the thermodynamic spectrum with perfect heat transfer for an isothermal process, $k = 1$.

With this substitution for ρ, the transient fairing pressure during the jettison process could be described as

$$p(t) = p_0 \left(\frac{V_0}{V(t)} \right)^k \exp\left(-ka \int_0^t \frac{A(t)}{V(t)} dt \right). \tag{5}$$

In Eq. (5), it is interesting to note that the polytropic exponent does not factor into the integral and may be treated as a time-dependent variable, independent of volumetric expansions or transient changes in vent area. Also, for a multiple-step jettison process, Eq. (5) describes each step of the process by suitable adjustment of the local time variable, where the initial pressure value for a subsequent step after the initial motion is given by conditions at the end of the previous step. Assuming volume and area changes are meant to be repeatable from one launch to the next, this means each step may be linked back to initial conditions and therefore should be linearly proportional with the initial pressure for a given event.

It should be noted that this lumped approach does not take into account angular variations in conditions around the LV main axis or possible localized flow features that may develop, therefore the description should be considered an approximate, aggregate response.

2.2 Constant Separation Rate Response

Eq. (5) is fairly general considering the assumptions. If transient volume and vent area increases due to fairing separation reasonably follow constant rates $\dot{V}$ and $\dot{A}$, then

$$V(t) = V_0 + \dot{V}t; \qquad A(t) = A_0 + \dot{A}t. \tag{6}$$

For purposes of illustration, assume nominal ascent fairing venting influence may be ignored relative to the jettison process, so $A_0 \approx 0$. Substitution of Eq. (6) expressions into Eq. (5) produces

$$\begin{aligned} p(t) &= p_0 \left(\frac{V_0}{V_0 + \dot{V}t} \right)^{k(t)} \exp\left(-k(t) a \int_0^t \frac{\dot{A}t}{V_0 + \dot{V}t} dt \right) \\ &= p_0 \left(\frac{V_0}{V_0 + \dot{V}t} \right)^{k(t)} \exp\left\{ -k(t) a \frac{\dot{A}}{\dot{V}} \left[t - \frac{V_0}{\dot{V}} \ln\left(1 + \frac{\dot{V}t}{V_0} \right) \right] \right\} \\ &= p_0 \left(\frac{V_0 + \dot{V}t}{V_0} \right)^{k(t)\left(a \frac{\dot{A}V_0}{\dot{V}^2} - 1 \right)} \exp\left(-k(t) a \frac{\dot{A}t}{\dot{V}} \right). \end{aligned} \tag{7}$$

For k = const., Eq. (7) indicates there is a natural exponential decay time constant $\tau \equiv \dot{V}/ka\dot{A}$, but its impact is obscured in the resulting pressure behavior by a power-law dependence on time as well.

3. PARAMETRIC ANALYSIS

In the analysis that follows, $\left(p_0, V_0, \dot{V}, \dot{A}, k\right)$ = (100 Pa, 300 m^3, 1000 m^3/s, 250 m^2/s, γ = 1.4) were chosen as a set of baseline parameters for exploring solutions in a parametric analysis. These are meant to be roughly representative of conditions for a large d = 5 m LV fairing at jettison. In addition, assume that the separation speed of the fairing halves being separated transversely from the LV thrust axis or axis of symmetry is $\dot{L}$ = 10 m/s. First, the overall Knudsen number Kn will be checked to determine the suitability of this analysis in terms of pressure.

3.1 Flow Regime Check

First, while it is recognized that the ensemble of gas acted upon by the receding fairing halves is not a steady environment, it is being treated this way approximately since the rate of fairing half separation ($\dot{L}$ = 10 m/s), is slow relative to molecular speeds at T_0 = 293 K (a_0 = 343 m/s; most probable speed $\sqrt{2a_0/\gamma}$ = 410 m/s).[3] Assuming hard sphere intermolecular cross section σ = 4.34e-19 m^2 represents typical interactions in air treated as a homogeneous gas, the mean free path length λ based on lumped number density n is given by[4]

$$\lambda = \frac{1}{\sqrt{2}n\sigma} = \frac{KT}{\sqrt{2}p\sigma}, \tag{8}$$

where Boltzmann constant K = 1.38e-23 J/K. When p = 1 Pa and $T \approx$ 293 K, λ = 6.6 mm.

Although the separation distance L between fairing halves producing p = 1 Pa will vary depending on other parameters, it appears safe to assume for the first 0.2 s or so that the gas will be in the continuum regime (Kn < 0.01 roughly speaking). Looking ahead to Fig. 3, the reader will notice that analytical results for baseline conditions indicate 1 Pa is reached at 0.17 s. If the payload envelope approaches that for the fairing (radius R = 2.5 m), then the distance between the two at 0.2 s would be L = 1.7 m, and $Kn \equiv \lambda/L$ < 0.004. This would be an upper bound estimate since smaller payloads would increase the physical length parameter in Kn from L to $L + \Delta r$.

3.2 Thermodynamic Process

Since fairing jettison is a rapid, highly dramatic process, early results using Eq. (7) assumed conditions did not allow for heat transfer and the expansion of gas from within the fairing could be considered isentropic ($k = \gamma$). Later however, observations from indirectly related testing using the NASA Goddard Space Flight Center Rapid Pumpdown System[5] to evacuate a thermal vacuum chamber indicated that the thermodynamic process relaxed from isentropic to isothermal conditions. Conditions matched well with a polytropic exponent that relaxed linearly from $k = \gamma$ to k = 1 over a finite period.

Although it is assumed this process is essentially isentropic, a linear relaxation transient was also applied to the fairing jettison model for the sake of generality. The following relationship was applied to Eq. (7), where the polytropic exponent would transit from isentropic to isothermal conditions linearly over a finite period t_r :

$$k(t) = \begin{cases} \gamma - \left[(\gamma - 1)(t/t_r)\right]; & t < t_r \\ 1; & t \geq t_r. \end{cases} \tag{9}$$

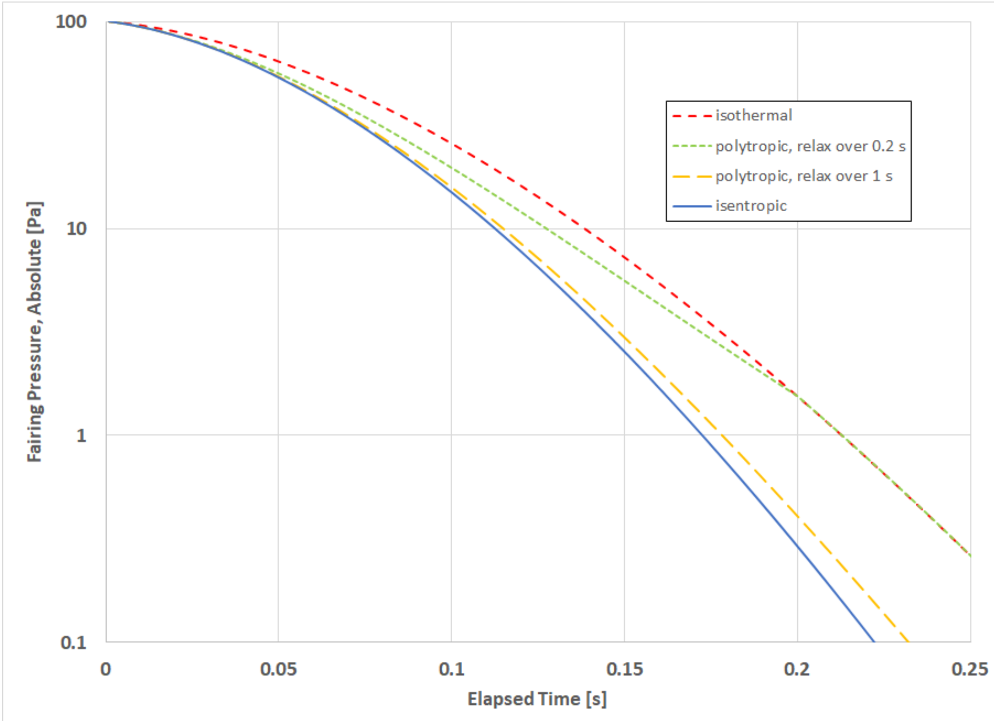

Figure 3. Fairing jettison response for nominal conditions (isentropic, solid curve), isothermal conditions, and cases featuring transient polytropic exponents.

Equation (9) was applied to Eq. (7) for a number of variations of polytropic exponent. Results are presented in Fig. 3 above. One may view the isentropic and isothermal case results as enveloping the range of possible responses for an actual jettison release from zero heat transfer to perfect heat transfer conditions throughout the process, respectively. An isentropic expansion produces the steepest pressure decay profile, while the isothermal process produces the shallowest. The intermediate curves attempt to demonstrate how relaxation might occur with heat transfer increasing from the isentropic limit.

3.3 Vent Area Rate

In this problem, investigating the influence of transient venting across the expanding area between a pair of receding fairing halves would appear to be linked to the rate of volume increase for this system, but one may still observe the influence of vent area rate separate from the volumetric expansion rate as it affects Eq. (7) in a parametric exercise. Figure 4 presents results for an isentropic expansion based on the nominal set of conditions as well as for slower and faster vent area rates.

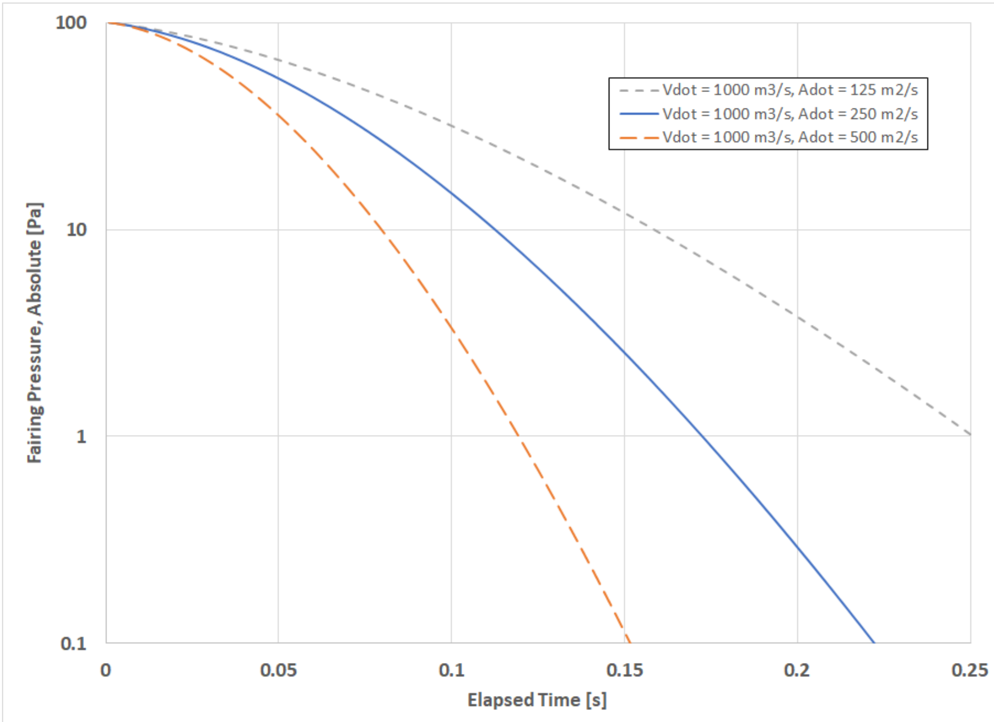

Figure 4. Isentropic fairing jettison pressure for nominal conditions (solid curve), as well as slower and faster rates.

Since Eq. (7) is highly non-linear, one notes a dramatic effect of venting rate on pressure decay results. At 0.15 s elapsed time, the pressure for a venting rate of $\dot{A}$ = 500 m²/s is two orders of magnitude below $\dot{A}$ = 125 m²/s results, so results are quite sensitive to this parameter. On the other hand, periods needed to reach a particular depleted value such as 1.0 Pa are only about doubled for these two cases. This is because the curves steepen dramatically with time throughout the continuum regime.

3.4 Volumetric Expansion Rate

Treated simply as a mathematical problem, one may vary the volumetric expansion rate $\dot{V}$ while keeping $\dot{A}$ fixed, although for an actual LV these parameters are probably linked and meant to be repeatable from launch to launch. Figure 5 compares results from the nominal set of isentropic conditions with cases where the volumetric expansion rates are doubled and halved.

It is interesting to note the curves vary much less from one another than the influence relative changes of $\dot{A}$ had shown in Fig. 4. Another surprising result in Fig. 5 is an apparent crossover point where pressure levels for any two different curves tend to intersect. For this to occur, one would ratio Eq. (7) with one set of conditions (subscript 1) to another version with the same variables except a different volumetric expansion rate (subscript 2). Then replace the left-hand side pressure ratio with the value of one to find the crossover time $\tilde{t}$. The following condition is reached:

$$\exp\left[ka\dot{A}\tilde{t}\left(\frac{1}{\dot{V}_1}-\frac{1}{\dot{V}_2}\right)\right] = V_0^{\,ka\dot{A}V_0\left(\frac{1}{\dot{V}_2^2}-\frac{1}{\dot{V}_1^2}\right)}\left(V_0+\dot{V}_1\tilde{t}\right)^{k\left(a\frac{\dot{A}V_0}{\dot{V}_1^2}-1\right)}\left(V_0+\dot{V}_2\tilde{t}\right)^{k\left(1-a\frac{\dot{A}V_0}{\dot{V}_2^2}\right)}. \tag{10}$$

Recognizing from earlier that Eq. (7) had an exponential time constant $\tau \equiv \dot{V}/ka\dot{A}$, Eq. (10) reduces to

$$\tilde{t} = \frac{\tau_1\tau_2}{\tau_2-\tau_1}\ln\left\{ V_0^{\,V_0\left(\frac{1}{\tau_2\dot{V}_2}-\frac{1}{\tau_1\dot{V}_1}\right)}\left(V_0+\dot{V}_1\tilde{t}\right)^{\left(\frac{V_0}{\tau_1\dot{V}_1}-k\right)}\left(V_0+\dot{V}_2\tilde{t}\right)^{\left(k-\frac{V_0}{\tau_2\dot{V}_2}\right)}\right\}. \tag{11}$$

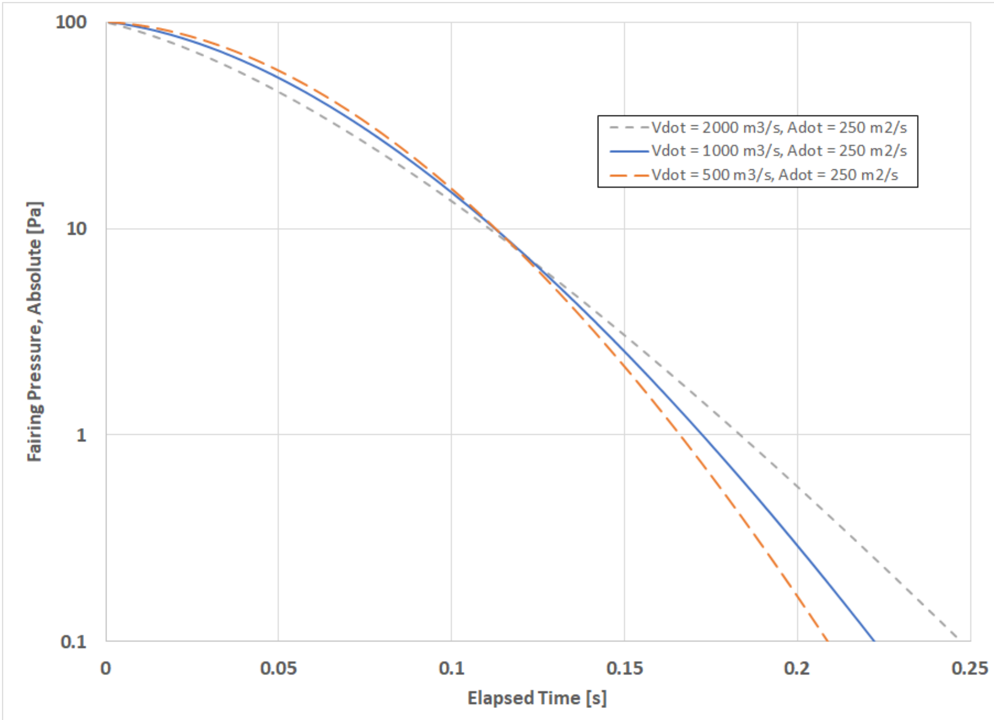

Figure 5. Isentropic fairing jettison pressure for nominal conditions (solid curve), along with slower and faster rates of volumetric expansion at fixed vent area rate.

Although computing $\tilde{t}$ where two fairing jettison pressure curves intersect involves iterating solutions on a rather unappealing recursive equation, the logarithmic dependence of the right-hand side indicates $\tilde{t}$ is a weak function of $\dot{V}$. This crossover time may result from the observation that pressure decreases due to two different mechanisms: one from the expanding volume, and another because the vent area rate increases. For a given initial volume, lower $\dot{V}$ levels lead to higher pressures early on. These higher pressures give rise to higher gas load potentials and greater venting later, ultimately resulting in steeper evacuation profiles relative to faster $\dot{V}$ cases.

4. EXAMPLE--PAYLOAD RESPONSE

Payloads within the fairing will develop overpressures relative to fairing conditions as jettison occurs. Beginning with Eq. (1) and assuming fixed volume V with no mass generation and fixed orifice-type venting area A_{eff},[6,7]

$$V\frac{d\rho}{dt} = -\dot{m} = -A_{eff}\sqrt{\frac{2\gamma}{\gamma-1}p\rho}\sqrt{\left(\frac{p_f}{p}\right)^{\frac{2}{\gamma}} - \left(\frac{p_f}{p}\right)^{\frac{\gamma+1}{\gamma}}}\ . \tag{12}$$

For polytropic conditions, $p \propto \rho^k$. In the example cases being considered where the payload volume and vent area are both much smaller than fairing attributes during jettison, one may consider simply assuming isothermal conditions and that payload contributions to the fairing environment may be ignored. With the understanding that attention is focused on the payload conditions in this section, fairing conditions will carry subscript *f*, and

$$\frac{dp}{dt} = -pa_0 \frac{A_{eff}}{V} \sqrt{\frac{2}{\gamma - 1}} \sqrt{\left(\frac{p_f}{p}\right)^{\frac{2}{\gamma}} - \left(\frac{p_f}{p}\right)^{\frac{\gamma+1}{\gamma}}} . \tag{13}$$

Transient payload pressure may be found by numerically integrating Eq. (13) over time using the fairing pressure profile as an input forcing function. A sonic constraint forms when $p_f / p < \left[2/(\gamma+1)\right]^{\frac{\gamma}{\gamma-1}}$. Below this value, the pressure ratio is replaced by the latter expression, and subsequent fairing pressure behavior does not affect payload venting.

A convenient, although imprecise way often employed to meet overpressure requirements is to specify a maximum volume to vent area ratio, such as V/A_{eff} = 2000 inches.[8] Reliance on such specifications are imprecise since Eq. (13) indicates that fairing evacuation behavior also plays a role in determining peak overpressure.

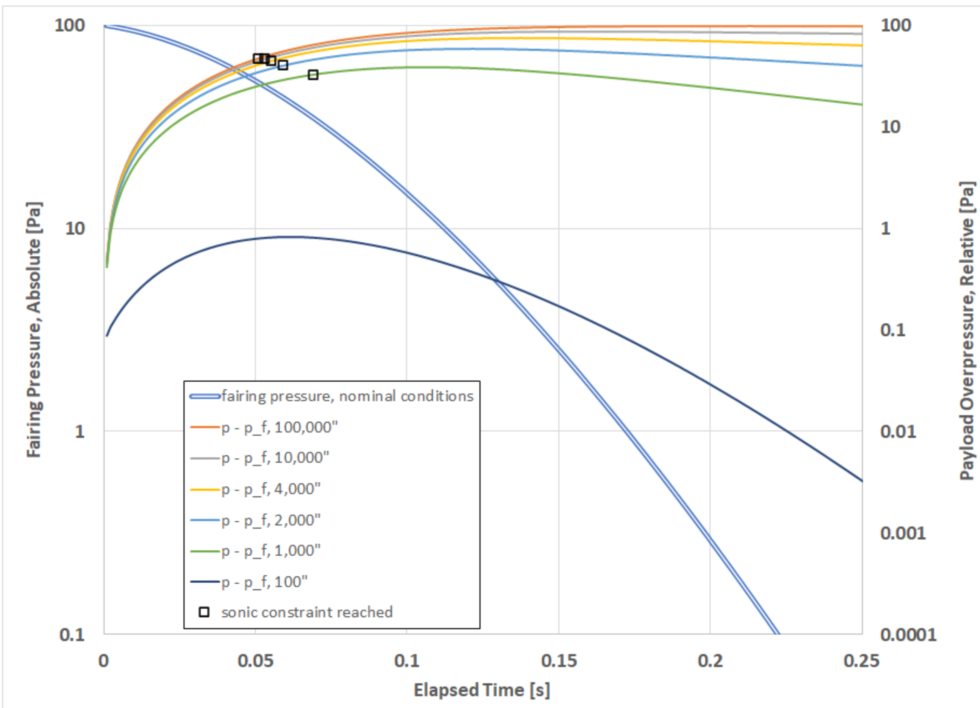

Figure 6. $V = 1$ m^3 payload overpressure responses due to baseline fairing jettison conditions.

Figure 6 presents results for a variety of V/A_{eff} values where $V = 1$ m^3. Overpressures associated with high V/A_{eff} ratios are essentially similar to assuming an instantaneous fairing depressurization, while lower V/A_{eff} ratio results indicate payload volumes that are able to relieve themselves a bit before reaching peak values. Results indicate ratios of 1000" and above cannot follow this example jettison pressure profile closely, and tend to reach sonic vent constraints before 70 milliseconds. At a ratio of 100,000", sonic conditions are reached essentially as soon as $p_f / p_{f,0} = \left[2/(\gamma+1)\right]^{\frac{\gamma}{\gamma-1}}$, indicating practically no venting occurred by that time (51 milliseconds for example conditions).

Conversely, a V/A_{eff} of 100" represents a square hole of length of about 63 cm (24.7") on a side for a vessel of 1 m^3, which generally might not be considered a realistic vent area when considerations of heat transfer and intrusion of energetic particles are taken into account for various spacecraft assemblies.

However, a square MLI blanket covering 1 m^2 with a thickness of ¼" could conservatively achieve V/A_{eff} =100" by having 15.5", or about ten percent of its 157.5" perimeter left unsealed. Coincidentally, this observation corresponds closely to GSFC practices already in existence for blankets of this size and proportions.[9]

5. CONCLUDING REMARKS

An analytical model has been developed to describe fairing conditions during jettison. Although it uses lumped parameters to describe initial physical conditions and to evaluate the jettison process, it is general in terms of characterizing the transient nature of volume and vent area expansion, as well as the thermodynamic process that also affects the pressure environment. While results should provide an envelope of possible overall pressure responses to this event, it cannot reveal angular dependence of expansion features around the LV main axis, nor can it discern local variations in behavior.

A parametric analysis was performed on a number of model variables for linearly increasing volumes and vent areas. Results indicated much greater sensitivity to vent area rates than changes in volumetric expansion rates, and for the latter that an approximately stable point occurs where different volumetric expansion rates will produce the same pressure at around the same time in the process.

The response for a hypothetical 1 m^3 payload volume or subassembly was predicted for a variety of vent areas using variations based on a common rule of thumb specification. Overpressure responses due to representative specifications of V/A_{eff} of 1000" or higher were found not to follow the fairing pressure very well, with sonic constraints being reached while the fairing pressure was at about thirty percent of its initial value or above. On the other hand, a representative MLI blanket may tend to follow fairing evacuation closely with volume to vent area ratios of 100", which may correspond to untaped portions of blanket edges of about ten percent.

6. ACKNOWLEDGEMENTS

MSW gratefully acknowledges support from NASA Contract NNG17CR69C and the efforts of Eve Wooldridge, NASA-GSFC Code 546, Michael Menzel, Code 590, and Allan Sherman, ATA Aerospace.

REFERENCES

[1] Anon., "James Webb Space Telescope Observatory Design Description Document," Northrop Grumman Systems Corporation, Doc. No. D42904 Rev. B, 5-5 (2017).
[2] Mather, J., "James Webb Space Telescope: Why are we building it like this?", NASA Goddard Space Flight Center, Doc. No. JWST-PRES-020901, 9 October 2012.
[3] Vincenti, W., and Kruger, C., *Introduction to Physical Gas Dynamics*, Robert E. Krieger Pub. Co., Malabar, FL, 14 (1982).
[4] Kennard, E., *Kinetic Theory of Gases*, McGraw-Hill Book Co., Inc., New York, 113, 149 (1938).
[5] Anon., "Environmental Test and Integration Facilities Handbook," NASA Goddard Space Flight Center, Code 549, NP-2013-4-021-GSFC, 59 (2013).
[6] Holman, J., *Experimental Methods for Engineers*, 4th ed., McGraw Hill, New York, 234-235 (1984).
[7] Karam, R., "RAE Spacecraft Venting," Fairchild Hiller Memo No. SESD-TH-0083, 3 July 1967.
[8] Anon., "Space Flight System Design and Environmental Test," ARC-STD-8070.1, NASA Ames Research Center, Section 3.1.1.6 (2018).
[9] Anon., "Design and Fabrication of Thermal Blankets," ManTech Intl. Corp. Doc. No. 09PC-W157 Rev. 1, 3 July 2003.